

A&A manuscript no.
(will be inserted by hand later)
Your thesaurus codes are:
09.16.1; 13.03.19.3; 10.05.1

**ASTRONOMY
AND
ASTROPHYSICS**

Measurements of $^{12}\text{C}/^{13}\text{C}$ in planetary nebulae: implications on stellar and Galactic chemical evolution

F. Palla¹, R. Bachiller², L. Stanghellini^{3,4*}, M. Tosi³, D. Galli¹

¹ Osservatorio Astrofisico di Arcetri, Largo E. Fermi 5, I-50125 Firenze, Italy

² Observatorio Astronómico Nacional (IGN), Campus Universitario, Apdo. 1143, E-2880 Alcalá de Henares (Madrid), Spain

³ Osservatorio Astronomico di Bologna, Viale Berti Pichat 6/2, I-40126 Bologna, Italy

⁴ Space Telescope Science Institute, 3700 San Martin Drive, Baltimore MD 21218, USA

Received date: 16 April 1999; accepted date: 8 November 1999

Abstract. We present the results of a study aimed at determining the $^{12}\text{C}/^{13}\text{C}$ ratio in two samples of planetary nebulae (PNe) by means of millimeter wave observations of ^{12}CO and ^{13}CO . The first group includes six PNe which have been observed in the $^{3}\text{He}^{+}$ hyperfine transition by Balser et al. (1997); the other group consists of 22 nebulae with rich molecular envelopes. We have determined the carbon isotopic ratio in 14 objects, 9 of which are new detections. The results indicate a range of values of $^{12}\text{C}/^{13}\text{C}$ between 9 and 23. We estimate the mass of the progenitors of the PNe of our sample and combine this information with the derived $^{12}\text{C}/^{13}\text{C}$ isotopic ratios to test the predictions of stellar nucleosynthesis models.

We find that the majority of PNe have isotopic ratios below the values expected from current standard asymptotic giant branch models in the mass range of interest. We suggest that the progenitors of the PNe must have undergone a non-standard mixing process during their red giant phase and/or asymptotic giant phase, resulting in a significant enhancement of the ^{13}C abundance in the surface layers. Our study confirms a similar behaviour inferred from spectroscopic observations of field population II stars and globular cluster giants, and extends it to the final stages of stellar evolution. Finally, we discuss the implications of our results on models of Galactic chemical evolution of ^{3}He and $^{12}\text{C}/^{13}\text{C}$.

Key words: planetary nebulae: general – radio lines: ISM – Galaxy: evolution

1. Introduction

In the PN phase, stars more massive than $0.8 M_{\odot}$ return to the ISM material that has been processed in the

Send offprint requests to: F. Palla

* Affiliated with the Astrophysics Division, Space Science Department of ESA

Correspondence to: palla@arcetri.astro.it

stellar interior. This matter mixes with the surrounding medium and modifies the original abundances of elements. The contribution of PNe to the Galactic chemical evolution is particularly important for ^{3}He which, together with deuterium, plays a fundamental role in testing the standard Big Bang nucleosynthesis model. While the evolution of deuterium is well understood, that of ^{3}He still encounters serious problems which cast doubts on the usefulness of this isotope as a test of Big Bang nucleosynthesis models (e.g. Galli et al. 1995; for a different opinion on deuterium see Mullan & Linsky 1999). Observations of ^{3}He toward PNe and HII regions have resulted in abundances that differ by almost two orders of magnitude: $^{3}\text{He}/\text{H} \sim 10^{-3}$ in PNe (Rood et al. 1992, Balser et al. 1997), and $^{3}\text{He}/\text{H} \sim 10^{-5}$ in HII regions (Balser et al. 1994, Rood et al. 1995). The latter value is also representative of the ^{3}He abundance in the presolar material (Geiss 1993) and the local ISM (Gloeckler & Geiss 1996). However, the abundance in PNe agrees with the predictions of standard stellar evolution models for stars of mass $1\text{--}1.5 M_{\odot}$ (see the review by Rood et al. 1998). The main question is then: if low-mass stars are net producers of ^{3}He and return it to the ISM during the PN phase, why don't we observe a much higher abundance in HII regions and in the solar system material, as all standard Galactic evolutionary models predict (see e.g. Tosi 1996)?

An interesting solution to this problem involves the existence of a nonstandard mixing mechanism (or Cool Bottom Processing, hereafter CBP) which operates during the red giant phase of stars with $M \lesssim 2 M_{\odot}$. In addition to decreasing the amount of ^{3}He in the stellar envelope, this process affects the abundances of other important elements, including carbon, as first suggested by Hogan (1995), Charbonnel (1995) and Wasserburg et al. (1995). In particular, the ratio of $^{12}\text{C}/^{13}\text{C}$ in the envelope is predicted to be much *lower* than in the standard case. For a $1 M_{\odot}$ star, the predicted ratio is about 5 against the standard value of 25–30 in the red giant branch (RGB) and of 20–40 in the asymptotic giant branch (AGB). However, the discrepancy becomes

larger for more massive stars where the $^{12}\text{C}/^{13}\text{C}$ ratio can reach ~ 100 in the AGB phase (Charbonnel 1995; Weiss et al. 1996; Forestini & Charbonnel 1997, hereafter FC; van den Hoek & Groenewegen 1997, hereafter HG; Marigo 1998; Boothroyd & Sackmann 1999, hereafter BS).

From an observational viewpoint, it is important to obtain accurate measurements of the isotopic ratio in those PNe where the ^3He abundance has been determined. Should these objects show a high value of $^{12}\text{C}/^{13}\text{C}$, then no modifications to the standard stellar models would be required. Otherwise, one has to invoke another selective process (mixing, diffusion etc.) that operates on some isotopes but not on ^3He . However, the number of PNe with ^3He measurements is small (e.g. Balser et al. 1999), whereas the suggested physical processes should be quite general and should affect the nucleosynthetic yields of all stars of mass less than $\sim 2 M_\odot$. Hence, it is critical to measure the carbon isotopic ratio in a sample of PNe as large as possible.

The molecular envelopes of PNe have been studied extensively at near infrared and millimeter wavelengths (see e.g. Kastner et al. 1996, Huggins et al. 1996, Bachiller et al. 1997). These observations have shown that massive envelopes ($\gtrsim 10^{-2} M_\odot$) containing a rich variety of molecular species are commonly found around PNe. CO is the most widely observed species, and the $^{12}\text{C}/^{13}\text{C}$ isotopic ratio has been measured toward several PNe (Bachiller et al. 1989, 1997; Cox et al. 1992). These initial studies have shown that the $^{12}\text{C}/^{13}\text{C}$ ratio is in the range 10–20.

Our project consists of two parts. In the first one, we have carried out high quality observations of ^{12}CO and ^{13}CO in six PNe that have been searched for ^3He emission. In the second run, a larger sample of nebulae with strong ^{12}CO line emission has been observed in the ^{13}CO lines in order to determine the isotopic ratio in PNe *without* ^3He measurements. Galli et al. (1997, hereafter GSTP) have argued that extra-mixing processes must be at work in more than 70% of low-mass stars ($M \lesssim 2 M_\odot$) in order to reconcile the predictions of the Galactic evolution of ^3He with the observational constraints. We set out this experiment to determine the isotopic ratio in a relatively large sample of PNe.

2. Observations

The observations were carried out with the IRAM 30-m telescope at Pico Veleta (near Granada, Spain) during two observing runs in November 1996 and May 1997. In the first one we observed the six PNe studied by Balser et al. (1997). The observations were made simultaneously in the $J = 2-1$ and $1-0$ lines of ^{12}CO . The strongest emitters were then observed in the ^{13}CO lines. In the second run we searched for ^{13}CO $J = 2-1$ and $1-0$ emission in 22 objects previously detected in ^{12}CO by Huggins et al. (1996). At the rest frequency of the $J = 2-1$ and $1-0$ ^{12}CO lines (near 115 and 230 GHz, respectively) the telescope beam-

size and efficiency are $24''$ and 0.6 (115 GHz) and $12''$ and 0.45 (230 GHz). The smaller beam size at 230 GHz, together with the small scale structure usually found in PNe and with the high intrinsic CO (2–1)/(1–0) line ratio, lead to observed 2–1/1–0 line ratios in the range 2–5 (Bachiller et al. 1993), meaning that the $J = 2-1$ line is much more effective for CO searches. The spectrometers used were two filter banks of 512×1 MHz channels, providing a spectral resolution of 1.3 km s^{-1} in the ^{12}CO 2–1 line, and 2.6 km s^{-1} in the ^{12}CO 1–0 line. Typical system temperatures were around 600 K at 115 GHz and 800–1000 K at 230 GHz. The spectra were calibrated with the standard chopper wheel method and are reported here in units of main-beam brightness temperature (T_{MB}).

3. Measuring the carbon isotopic ratio from millimeter wave observations

Molecular line observations at mm-wavelengths provide a powerful method to estimate the $^{12}\text{C}/^{13}\text{C}$ ratio in PNe. In particular, the $^{12}\text{CO}/^{13}\text{CO}$ ratio should faithfully reflect the atomic $^{12}\text{C}/^{13}\text{C}$ ratio, since the mechanisms which could alter the $^{12}\text{CO}/^{13}\text{CO}$ ratio are not expected to be at work in PNe. In fact, the kinetic temperature in PN envelopes (25–50 K) is high enough that isotopic fractionation should not operate. Also, selective photodissociation is expected to be compensated by the isotope exchange reaction $^{12}\text{CO} + ^{13}\text{C}^+ \rightarrow ^{13}\text{CO} + \text{C}^+$ which is faster than the ^{13}CO photodestruction in PN envelopes (e.g. Likkel et al. 1988). However, although the $J = 1-0$ and $J = 2-1$ lines of ^{12}CO have been extensively observed in PNe (e.g. Huggins et al. 1996), very few observations of the ^{13}CO lines are available and the value of the isotopic ratio is presently poorly known.

In order to estimate the $^{12}\text{CO}/^{13}\text{CO}$ isotopic ratio, one needs to make a number of approximations. First, we assume that the emitting regions fill the antenna beams in the lines of both molecules, or that the filling factor is the same (in the case of an extended clumpy medium). Second, we assume that the rotational levels are thermalized at a representative uniform temperature of 25 K (see e.g. Bachiller et al. 1997). Thermalization is indeed a reasonable assumption for ^{12}CO and ^{13}CO , since the dipole moment is quite small (about 0.1 Debye). Third, if we assume that the emission is optically thin for both the ^{12}CO and ^{13}CO lines, then the $^{12}\text{CO}/^{13}\text{CO}$ column density ratio is given by the ratio of the integrated intensities. We will discuss below the uncertainties introduced by this approach in the derived isotopic ratios.

4. Results

4.1. PNe with ^3He measurements

The results of the observations are given in Table 1 where we list the PN name, the intensities I_{21} of the ^{12}CO and ^{13}CO $J = 2-1$ lines and the derived isotopic ratio. The

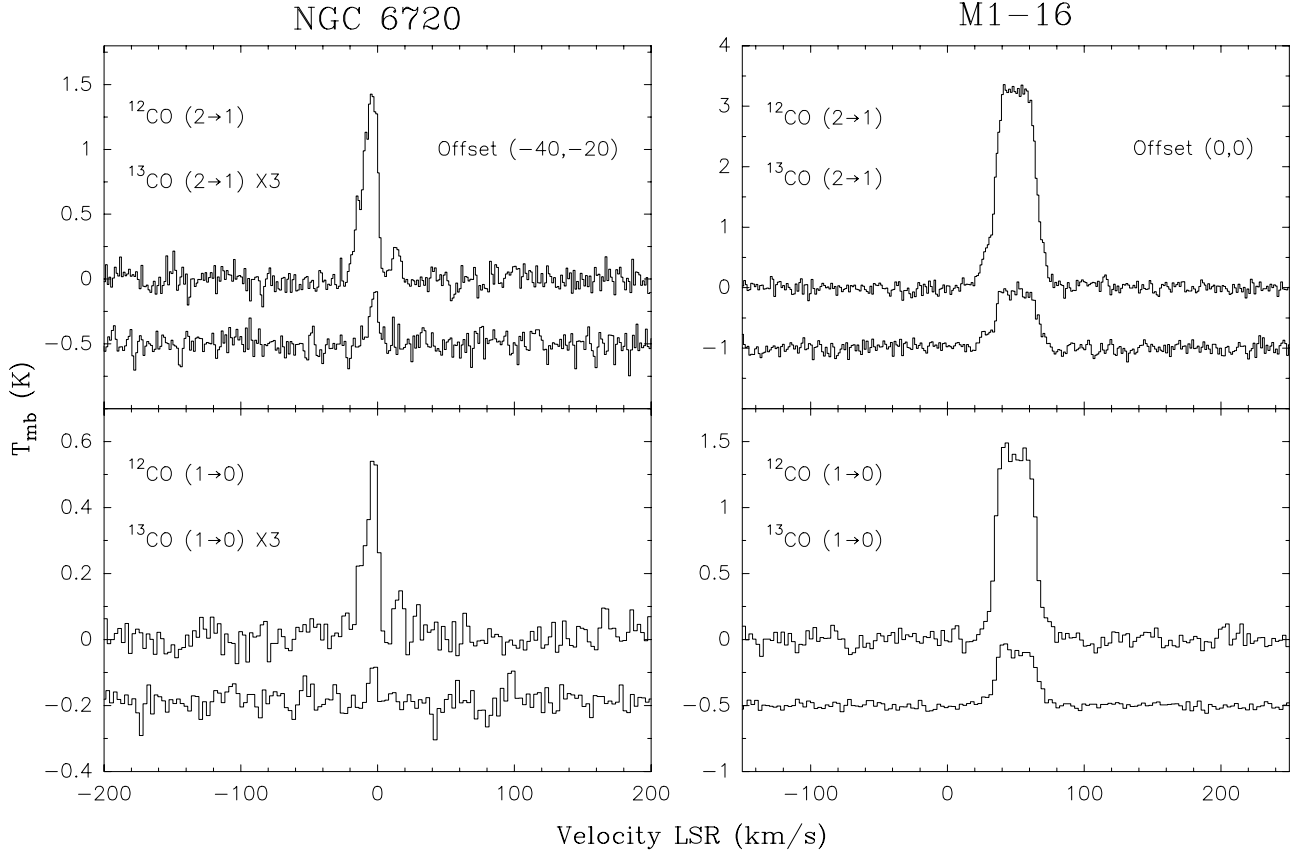


Fig. 1. CO emission in PNe. Two examples are shown from the sample of PNe with (left) and without (right) ^{3}He measurements. The offset in arcsec from the central PN is also indicated. The stronger $J = 2-1$ transitions are shown in the upper panels, while the $J = 1-0$ transitions in the bottom panels. The isotopic lines are detected in both cases.

sample of the six PNe studied in ^{3}He shows little emission in CO: with the exception of NGC 6720, the values of I_{21} represent upper limits to the intensity and have been estimated from the line widths deduced from the expansion velocities listed in the catalog of Acker et al. (1992).

Bachiller et al. (1989) detected an extended molecular envelope in NGC 6720, the Ring nebula. The CO emission reveals a clumpy ring, resembling to that of the ionized nebula. We observed the $J = 2-1$ and $1-0$ lines of ^{13}CO in three positions and detected emission in all cases. Fig. 1 shows the spectra of the four CO and ^{13}CO lines observed toward the strongest peak in the molecular envelope (offset $[-40'', -20'']$ from the central position). The measured isotopic ratio toward this position, where the S/N is the highest, is $^{12}\text{C}/^{13}\text{C} = 22$. This value is in agreement with a previous estimate of Bachiller et al. (1997) and with the values obtained toward the two positions with lower S/N spectra. Thus, our data provide no evidence for variations of the isotopic ratio across the nebula.

We have also detected a line around the ^{12}CO $J = 1-0$ frequency in the central position of NGC 6543, but we

Table 1. CO results for PNe observed in ^{3}He

PN Name	$I_{21}(^{12}\text{CO})$ (K km s^{-1})	$I_{21}(^{13}\text{CO})$ (K km s^{-1})	$^{12}\text{C}/^{13}\text{C}$
IC 289	<0.90		
NGC 3242	<0.16		
NGC 6543	<0.19		
NGC 6720	20.0	0.9	22
NGC 7009	<0.12		
NGC 7662	<0.12		

failed to detect the $J = 2-1$ line at relatively low levels. This indicates that the line near the $J = 1-0$ frequency is probably not due to CO. It is interesting to recall that the H38 α recombination line is only separated by 3 MHz (7.8 km s^{-1}) from the ^{12}CO $J = 1-0$ line. As discussed in Bachiller et al. (1992), the H38 α line can dominate the emission around the ^{12}CO $J = 1-0$ frequency in some nebulae with little or no molecular gas. We believe that this is the case in the central position of NGC 6543.

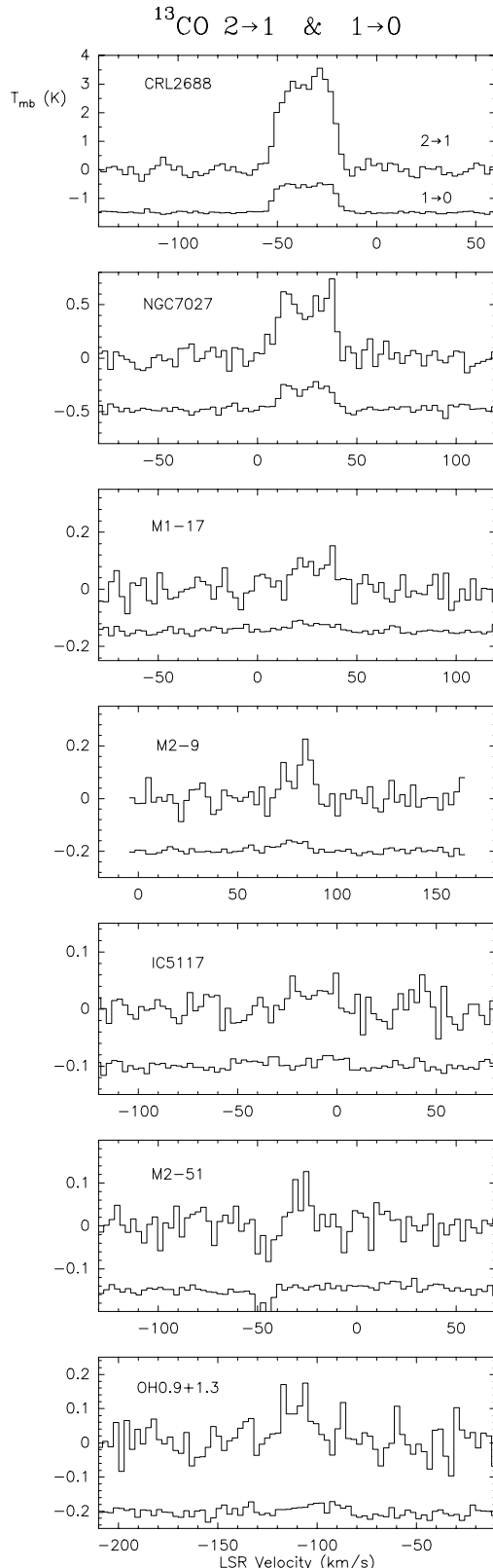


Fig. 2. ^{13}CO $J = 2-1$ and $1-0$ spectra observed toward the central position of the PN identified in the upper left corner of each panel.

Table 2. CO results for PNe not observed in ^3He

PN Name	$I_{21}(\text{CO})$ (K km s^{-1})	$I_{21}(\text{CO})$ (K km s^{-1})	$^{12}\text{C}/^{13}\text{C}$
NGC 7027	448.7	17.3	25 [†]
NGC 2346	14.2	0.58	23
NGC 7293	17.5	1.8	9
NGC 6781	28.4	1.72	20
M 1-16	109.0	32.3	3 [†]
M 1-17	66.2	3.2	22
M 2-9	3.3	2.0	2 [†]
M 2-51	33.1	2.3	15
M 4-9	32.2	1.8	18
CRL 2688	312.5	112	3 [†]
CRL 618	182.2	41.2	4 [†]
OH 09+1.3	5.0	2.5	2 [†]
IC 5117	19.6	1.4	14
NGC 7008	1.8	≤ 0.15	≥ 12
NGC 6853	6.9	≤ 0.15	≥ 46
M 1-13	22.2	≤ 1.5	≥ 15
BD+30°3639	4.7	≤ 1.1	≥ 4

[†] lower limit

4.2. PNe without ^3He measurements

The parameters of the detected sources and the derived isotopic ratios are listed in Table 2. We have also included in this table data for NGC 2346, NGC 7293, NGC 6781, M 4-9, and CRL 618 from previous observations by Bachiller et al. (1989, 1997). The spectra of the remaining PNe are shown in Fig. 1 (for M 1-16) and in Fig. 2. In four cases (NGC 7008, NGC 6853, M 1-13, BD+30°3639) we obtained tentative detections in the ^{13}CO lines, or only crude upper limits could be derived.

The assumption of optically thin emission used to determine the isotopic ratio is likely to be accurate in the case of evolved nebulae like the Ring, the Helix, NGC 2346, etc. In fact, Large-Velocity-Gradient (LVG) models confirm that the ^{12}CO and ^{13}CO line emission is optically thin in these cases. On the other hand, the same assumption is not appropriate for the CO lines in young objects such as CRL 2688, CRL 618, NGC 7027, and M 1-16. In such cases, the derived CO column densities and $^{12}\text{CO}/^{13}\text{CO}$ column density ratios represent only approximate lower limits.

One could also have weak emission arising from small optically thick clumps very diluted within the ^{12}CO and ^{13}CO beams. This could be the case in some compact CO envelopes such as the Butterfly nebula, M 2-9. The CO in M 2-9 is concentrated in an expanding clumpy ring which has a mean diameter of 6 arcsec (Zweigle et al. 1997). Individual clumps in this ring have sizes < 4 arcsec. The weakness of the ^{12}CO and ^{13}CO lines we observe could be due to the important dilution of such small clumps within the 30-m beam. The clumps could be optically thick in CO, and the reported $^{12}\text{CO}/^{13}\text{CO}$ intensity ratio would

just represent a lower limit to the abundance ratio in these compact PNe.

In the case of extended PNe (e.g. NGC 6720, NGC 2346, NGC 7293), the assumption of optically thin CO 2–1 emission is based on detailed studies of individual nebulae which show that the intrinsic 2–1/1–0 line intensity ratio is typically >2 (Bachiller et al. 1989, 1993; Huggins et al. 1996). Such high ratios imply that the emission is optically thin, and that the excitation temperature is $T_{\text{ex}} \gtrsim 10$ K. In this approximation, and assuming homogeneous excitation conditions along the line of sight, the column density in the $J=2$ level is proportional to the observed 2–1 line intensity. Moreover, the relative population of the $J=2$ level is quite insensitive to the value of the excitation temperature for the typical conditions of PNe. The total CO column densities determined in this way are correct for T_{ex} in the range from 7 to 77 K, and are within a factor of 2 over the range from 5 to 150 K, which should cover most PNe. In any event, because of the similar dipole moments, the excitation temperature should be the same for both CO and ^{13}CO . Then, if the excitation conditions do not vary along the line of sight, the isotopic ratios are independent of T_{ex} .

The major source of uncertainty for these extended nebulae is thus related to the observational procedures. The calibration of our observations is accurate within 20%, but small differences in the filling factor for the different spectral lines could increase the uncertainty of the measured isotopic ratios up to a factor ~ 1.5 . As Table 2 shows, in the extended PNe where ^{13}CO is well detected (NGC 6720, NGC 2346, NGC 7293, NGC 6781, M 4-9, and M 2-51) the values of the isotopic ratios are in the range 9 to 23, to within a factor of ~ 1.5 . Such values are thus significantly lower than the Solar System value of 89, and appear to be consistent with those derived in AGB stars, as we shall discuss in Sect. 6.1.

5. Mass estimate of the progenitors of the PNe

In order to compare the observed isotopic ratios with the predictions of stellar evolutionary models, we must estimate the mass of the progenitors stars of the PNe. For the present samples, we have followed the procedure adopted in GSTP, consisting of the following steps.

(1) We assign to each nebula the best measured distance (or an average of available distances), the $\text{H}\beta$ flux, the HeII flux at 4686 Å, the angular size, and the B and V stellar magnitudes. Using these parameters, we calculate the effective temperature and luminosity via the Zanstra method (Kaler 1983).

(2) By locating the central star in the $\log T_{\text{eff}} - \log L$ plane, we derive its mass (M_{CS}) from comparison with a set of evolutionary tracks (Stanghellini & Renzini 1993).

(3) Using the initial mass–final mass relation, we compute the progenitor mass, that is the stellar mass on the main sequence (M_{MS}).

The stellar properties adopted for the PNe detected in ^{13}CO and the derived values of the progenitor mass are given in Table 3. Details on the individual objects are given in the Appendix.

Let us examine the uncertainty involved in the final mass calculations. Estimates of the stellar temperature and luminosity given in Table 3 are affected by errors in magnitudes, fluxes, diameters and extinctions. However, these quantities are usually determined with good accuracy ($\sim 5 - 20\%$), so that the uncertainty in the derived mass of the central stars does not exceed $\sim 15\%$, or $\sim 0.02 M_{\odot}$. The values given in the table do not include errors on the distances to the PN, which can be intrinsically high (up to 50%) but are difficult to estimate on an individual basis.

To infer the main sequence masses, we have used the initial mass–final mass relation given by Hervig (1996). This relation differs from that of Weidemann (1987) adopted in GSTP. We preferred Hervig's prescription since it is based on reliable observations of cluster white dwarfs, although the formal errors on the final mass are still substantial, and can amount to about $0.1 M_{\odot}$. Since we derive initial masses from final masses, the errors on the former quantity can be even larger. Quantitatively, we assign a formal error to the main sequence mass of $\Delta M_{\text{MS}} \simeq 1.5 M_{\odot}$ for low values of the initial mass ($M_{\text{MS}} < 2 M_{\odot}$), and a smaller error ($\Delta M_{\text{MS}} \simeq 0.75 M_{\odot}$) for higher masses. This difference is due to the change of the slope of the initial mass – final mass relation at about $2 M_{\odot}$: smaller masses are more sensitive to the adopted relation, and the uncertainty is correspondingly larger.

6. Implications

6.1. Implications on stellar nucleosynthesis

How do we interpret our results on the $^{12}\text{C}/^{13}\text{C}$ ratios in the framework of stellar nucleosynthesis? To help answering this question, we combine the information provided by the observed $^{12}\text{C}/^{13}\text{C}$ isotopic ratios with the mass estimates of the progenitors of the PNe, and with the predictions of some representative stellar nucleosynthesis models.

Since the formation of a PN takes place at the end of the AGB phase, the significant comparison is between the observed abundances and those predicted for the stellar ejecta at the AGB tip. Unfortunately, no stellar nucleosynthesis models up to these late phases are available in the literature for stars experiencing deep-mixing. For example, the calculations of Boothroyd & Sackmann (1999) allow to derive the mass dependence of the $^{12}\text{C}/^{13}\text{C}$ ratio on the stellar surface at the tip of the red giant branch both for the standard case and in the presence of extra-mixing. The standard models indicate that the isotopic ratio has approximately a constant value of 20–23 between $M = 2$ and $4 M_{\odot}$, and then increases steadily at lower masses

Table 3. Properties of individual PNe detected in ^{13}CO

#	PN Name	$\log T_{\text{eff}}$ (K)	$\log L$ (L_{\odot})	D (kpc)	M_{CS} (M_{\odot})	M_{MS} (M_{\odot})
1	NGC 7027	5.28 ± 0.02	3.66 ± 0.03	0.88	0.67 ± 0.03	2.6
2	NGC 2346	4.76 ± 0.01	3.80 ± 0.04	0.90	0.63 ± 0.02	2.3
3	NGC 7293	5.03 ± 0.01	2.03 ± 0.03	0.28	0.60 ± 0.03	2.6
4	NGC 6781	4.99 ± 0.03	2.94 ± 0.09	1.57	0.55 ± 0.02	1.0
5	M 1-16	4.91 ± 0.03	3.36 ± 0.14	5.43	0.56 ± 0.02	1.0
6	M 1-17	4.97 ± 0.03	2.89 ± 0.11	7.36	0.55 ± 0.05	1.0
7	M 2-9	> 4.65	> 2.54	1.32	(*)	> 2
8	M 2-51	5.06 ± 0.06	2.20 ± 0.15	1.92	0.63 ± 0.09	2.3
9	M 4-9	> 4.85	> 0.18	1.71	(*)	
10	CRL 2688					> 1.3
11	CRL 618	> 4.48	> 1.11	2.81	(*)	
12	OH 09+1.3					8.0
13	IC 5117	4.95 ± 0.03	3.31 ± 0.12	2.10	0.56 ± 0.02	1.0

(*) no HeII, no Zanstra analysis possible

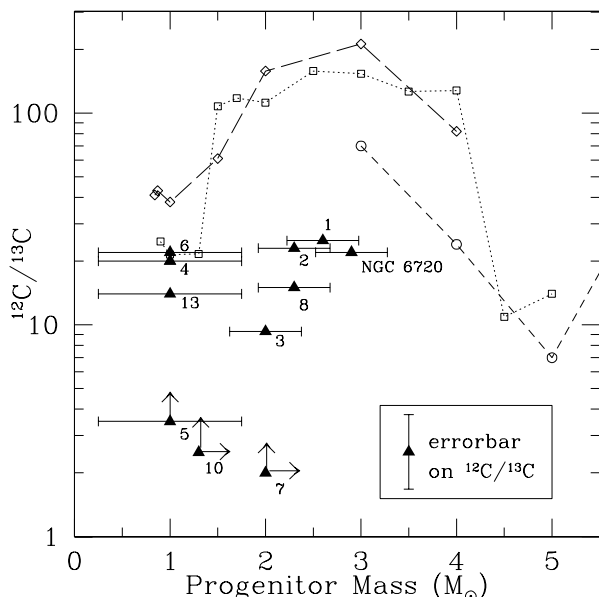


Fig. 3. $^{12}\text{C}/^{13}\text{C}$ versus progenitor mass of the PNe detected in CO. The filled triangles are the measured PNe, labelled as in Table 3. The uncertainty on the mass is described in the text. The error bar on the derived $^{12}\text{C}/^{13}\text{C}$ ratio is shown in the lower right corner. The three curves are the predicted $^{12}\text{C}/^{13}\text{C}$ ratios in the *ejecta* of stars at the tip of the asymptotic giant branch (AGB). The *dotted* curve is from van den Hoek & Groenewegen (1997), the *dashed* curve is from Forestini & Charbonnel (1997), and the *long-dashed* curve is from Marigo (1998). All curves are for solar metallicity.

up to about 28–30 with a small dependence on the stellar metallicity. In the case of extra mixing, the $^{12}\text{C}/^{13}\text{C}$ ratio displays a sharp drop below $\sim 2 M_{\odot}$, reaching values of

5–10 at $\sim 1 M_{\odot}$. Similar results have also been obtained by Charbonnel (1994) and Denissenkov & Weiss (1996).

In Fig. 3 we show the distribution of the measured $^{12}\text{C}/^{13}\text{C}$ ratios in 11 PNe, together with the theoretical values in the ejecta of stars at the tip of the AGB phase. The different curves refer to the models computed in the standard case with no mixing and solar metallicity by FC, HG, and Marigo (1998). Fig. 3 indicates that over the mass interval between 1.5 and 4 M_{\odot} the predictions of the HG and Marigo models are in good agreement with each other and indicate a roughly constant value of $^{12}\text{C}/^{13}\text{C} \sim 100$. The models of FC show significantly lower ratios at 3 and 4 M_{\odot} , but have the same qualitative behavior. These results are well understood in terms of the nucleosynthesis occurring during the thermally pulsating AGB phase. In fact, a major phase of ^{12}C enrichment of the convective envelope results from the penetration of the convective tongue during thermal pulses (see the discussion in, e.g., FC and HG). At the same time, ^{13}C is partially burnt through the $^{13}\text{C}(\alpha, n)$ reaction at the bottom of the inter-shell region during the inter-pulse phase, as first suggested by Straniero et al. (1995). The combination of these two effects accounts for the high $^{12}\text{C}/^{13}\text{C}$ ratio in this mass range. On the other hand, more massive AGB stars experience hot bottom burning that progressively leads the $^{12}\text{C}/^{13}\text{C}$ ratio close to its equilibrium value (~ 4 –5).

Despite the uncertainties in our measurements, it appears that the standard models produce $^{12}\text{C}/^{13}\text{C}$ in excess of the values observed in our objects. The only exception is for the two lowest mass stars (0.9 and $1.0 M_{\odot}$) computed by HG which agree with the ratios measured in M1-17 and NGC 6781. Although Fig. 3 indicates a marked discrepancy between observed and theoretical values, one should be aware of the sensitivity of the predicted yields on the model assumptions. In particular, the isotopic ratios (not only $^{12}\text{C}/^{13}\text{C}$) depend rather strongly on the adopted mass loss rate during the AGB phase, on the third

dredge-up efficiency, and on stellar metallicity. Their combined effects have been thoroughly discussed by FC and HG and need not to be repeated here. In general, a shorter phase of mass loss and/or lower mass loss rates tend to decrease the surface $^{12}\text{C}/^{13}\text{C}$ ratio. However, a more efficient convective penetration results in a higher pollution of the envelope from pulse to pulse and a higher $^{12}\text{C}/^{13}\text{C}$ ratio. Finally, stars with initial metallicities lower than solar yield higher $^{12}\text{C}/^{13}\text{C}$ ratios.

Returning to Fig. 3, we see that several PNe lie in the region of the diagram with low $^{12}\text{C}/^{13}\text{C}$ and low mass. For these objects we should expect the standard models to become inaccurate insofar as they neglect the possible occurrence of mixing mechanisms of non-convective origin which can alter the composition of the stellar ejecta. Low values of the carbon isotopic ratio have also been measured in field population II stars and in globular cluster giant (e.g. Sneden et al. 1986; Gilroy & Brown 1991; Piłachowski et al. 1997) and have provided the motivation to introduce extra-mixing processes in the standard evolution (e.g. Charbonnel 1995). Recently, Charbonnel & do Nascimento (1998) find that more than 90% of a sample of 191 field and cluster red giants presents carbon isotopic ratios inconsistent with those predicted by standard nucleosynthesis.

The observational situation in AGB stars is less clear, because of the extreme sensitivity of the determination of isotopic ratios on excitation temperatures and model atmospheres. For example, Greaves & Holland (1997) have measured a $^{12}\text{C}/^{13}\text{C}$ ratio varying between 12 and 36 in a sample of 9 carbon stars with high mass-loss rates ($\sim 10^{-5} M_{\odot} \text{ yr}^{-1}$), in accordance with similar results previously obtained by Wannier & Sahai (1987) on seven other carbon stars. On the other hand, Lambert et al. (1986) measured the $^{12}\text{C}/^{13}\text{C}$ ratio in 30 cool carbon stars and found values between 30 and 70. More recently, Ohnaka & Tsuji (1996) report ratios between 20 and 30 for 24 N-type carbon stars in common with the sample of Lambert et al. (1986). These values are about a factor of 2 smaller than those derived by Lambert et al. (see however the discussion in de Laverny & Gustafsson 1998 and Ohnaka & Tsuji 1998), but are consistent with those found for our PN sample. If these samples are representative of the population of both carbon stars and PNe, the low $^{12}\text{C}/^{13}\text{C}$ ratios provide strong indication that most stars should experience some extra-mixing and deplete ^{12}C with respect to ^{13}C . According to this conjecture, it appears that in order to match the observations, *more realistic stellar models should include additional physical processes to avoid too large $^{12}\text{C}/^{13}\text{C}$ ratios throughout the latest stages of stellar evolution*.

6.2. Implications on Galactic chemical evolution

Theoretical models predict that stars with low values of $^{12}\text{C}/^{13}\text{C}$ should also have low ^3He abundances. In GSTP,

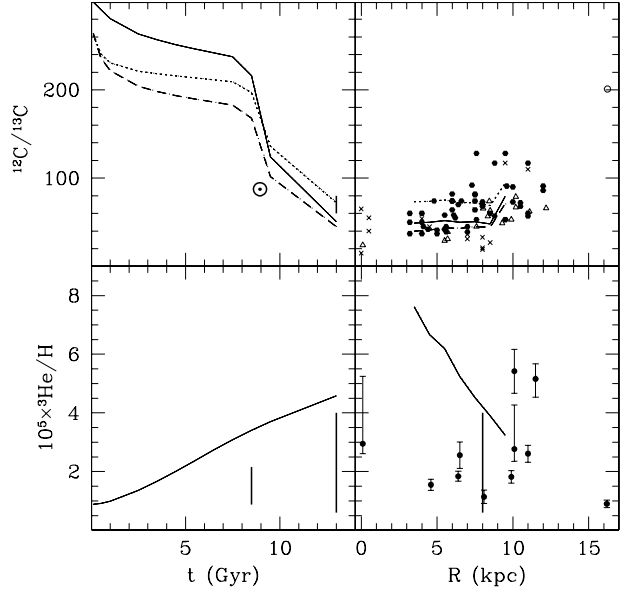


Fig. 4. Evolution of $^{12}\text{C}/^{13}\text{C}$ and ^3He as a function of time for the solar neighborhood and as a function of Galactocentric radius at the present time. Standard case with no extra mixing. The three curves show the results obtained using the yields for intermediate-mass stars by FC (*solid*), by HG (*dotted*), and by BS (*dashed*). The observational data for $^{12}\text{C}/^{13}\text{C}$ are from: Anders & Grevesse (1989); Henkel et al. (1980); Gardner & Whiteoak (1981); Henkel et al. (1982); Henkel et al. (1985), Langer & Penzias (1993); Wouterloot & Brand (1996). The data on ^3He are from Geiss (1993), Gloeckler & Geiss (1996) and Rood et al. (1995).

we estimated that to obtain consistency between the observed ^3He abundances and chemical evolution models, the majority of the Galactic PNe (>70%) should have a $^{12}\text{C}/^{13}\text{C}$ ratio well below the standard value. In this section we test this suggestion using the constraint provided by the $^{12}\text{C}/^{13}\text{C}$ observations in PNe. Chemical evolution models offer the adequate tool to follow simultaneously the evolution of $^{12}\text{C}/^{13}\text{C}$ and ^3He over the Galactic lifetime.

In Figs. 4 and 5 we show the evolution of $^{12}\text{C}/^{13}\text{C}$ and ^3He as a function of time in the solar neighborhood (Galactocentric radius $R = 8 \text{ kpc}$), and as a function of R at the present time ($t = 13 \text{ Gyr}$), as predicted by models described by Dearborn et al. (1996) and Sandrelli et al. (1998). The two figures correspond to different assumptions on the fraction of low-mass stars experiencing deep mixing in the RGB phase. In both cases, the Galactic evolution of the various isotopes has been computed assuming metallicity-dependent yields. In the upper panels, the solid line corresponds to models adopting the ^{12}C and ^{13}C yields from BS for stars in the mass range $0.8 - 2.5$

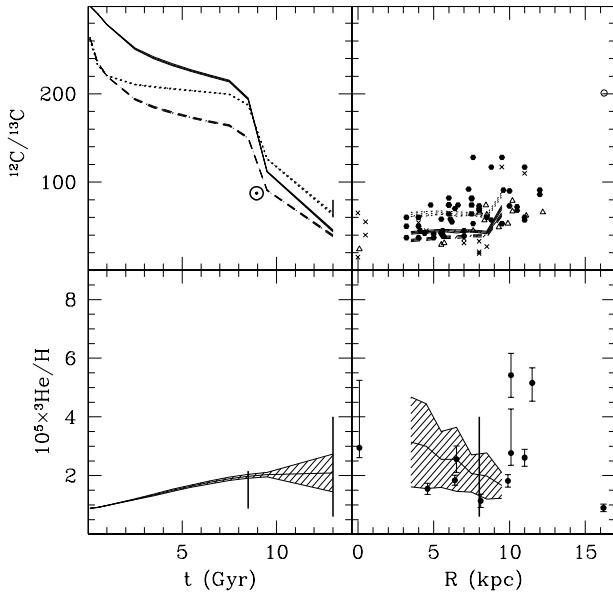


Fig. 5. Evolution of $^{12}\text{C}/^{13}\text{C}$ and $^{3}\text{He}/\text{H}$ as a function of time for the solar neighborhood and as function of Galactocentric radius at the present time. Case with mixing in 90% of low mass stars. Symbols and observational data are as in Fig. 4.

M_{\odot} , from FC in the range $3 - 6 M_{\odot}$, and from Woosley & Weaver (1995) for massive stars. The dotted and dashed lines display the results obtained using the same yields as before, except for stars in the mass range $3 - 6 M_{\odot}$, where the HG and BS yields, respectively, are adopted. The calculations by BS are the only ones that provide the ^{12}C and ^{13}C yields for both the standard and the CBP cases. For ^{3}He , the standard yields are taken from Dearborn et al. (1996) and the CBP yields from BS.

The behaviour of ^{3}He is typical of the elements produced mainly by low-mass, long-lived stars. ^{12}C is a primary element produced by stars of any mass and available for Galactic enrichment already after the explosions of the first massive objects. ^{13}C is mostly secondary and its bulk abundance is due to intermediate-mass stars. Therefore, the enrichment of this element in the ISM occurs later than that of ^{12}C . This delay causes the decrease of $^{12}\text{C}/^{13}\text{C}$ visible in Figs. 4 and 5. The positive radial gradient of $^{12}\text{C}/^{13}\text{C}$ is also due to the different mass intervals of stars that are producers of the carbon isotopes, and to the higher star formation activity in the inner Galactic regions, independent of the stellar initial mass function. All these effects combined make the relative proportion of ^{13}C over ^{12}C producers increasingly higher for decreasing Galactocentric distances.

Fig. 4 shows the standard case with no deep mixing, whereas the results with CBP in 90% of stars randomly chosen in the mass range $M \lesssim 2.5 M_{\odot}$ are displayed in

Fig. 5. The hatched regions represent the range of abundances resulting from 50 different cases for the random sorting. As already discussed by GSTP, the overall enrichment of ^{3}He is very sensitive to the assumptions on deep mixing. On the contrary, the variation of $^{12}\text{C}/^{13}\text{C}$ is marginal, since most of ^{12}C and ^{13}C is produced by stars more massive than $2.5 M_{\odot}$ which are not affected by deep mixing processes. Thus, altering the amount of ^{12}C and ^{13}C released by low-mass stars leads to smaller variations in the resulting abundances. For these reasons, the Galactic evolution of ^{3}He is an excellent indicator of the fraction of low-mass stars which should undergo CBP, but that of $^{12}\text{C}/^{13}\text{C}$ is not. From Figs. 4 and 5, one can see that the fraction required to reproduce the observed pattern of ^{3}He abundances is up to 90%, in agreement with the finding of Charbonnel & do Nascimento (1998).

As for $^{12}\text{C}/^{13}\text{C}$, the predicted abundance distributions with time and with Galactocentric distance are roughly consistent with the data regardless of the occurrence of extra-mixing. The $^{12}\text{C}/^{13}\text{C}$ ratio in the Sun cannot be accurately reproduced, and the radial gradient is flatter than the observed one (as deduced from measurements in molecular clouds), independently of the adopted percentage of stars undergoing CBP. Using the yields of FC and BS leads to a better fit of the solar value and to the present distribution of $^{12}\text{C}/^{13}\text{C}$ in the inner Galactic regions. On the other hand, the models of HG reproduce the local ISM ratio. In all cases, the fraction of low-mass stars experiencing deep mixing does not affect significantly the overall results of the chemical evolution models. Of course, deep mixing alters the values $^{12}\text{C}/^{13}\text{C}$ in low-mass stars, but the Galactic evolution of ^{12}C and ^{13}C is mainly governed by stars in which this process is not expected to take place.

7. Prospects for future observations

One of the main goals of our study was the determination of the isotopic ratio in NGC 3242, the best object for testing the mixing hypothesis since the ^{3}He measurements are very reliable and the progenitor mass is in the range where extra mixing should occur (see also the discussion in Rood et al. 1998). However, the high sensitivity of our observations and the fact that we searched for CO emission across the whole circumstellar shell imply that CO is absent in the nebula. We therefore conclude that the isotopic ratio cannot be determined in this important object by means of millimeter line observations. The lack of a molecular envelope around NGC 3242 can be a consequence of the low-mass of the progenitor. It is well known that the transition from the AGB phase to the PN stage is slow for low-mass stars and therefore the gas remains exposed to ionizing and dissociating radiation for a longer time than in the case of more massive stars.

This behavior is consistent with the fact that the most massive object of our sample, NGC 6720, indeed has a rich molecular envelope. Unfortunately, NGC 6720 has an esti-

mated progenitor mass of $\sim 2 M_{\odot}$, quite close to the limit where the nonstandard mixing mechanism is expected to significantly affect the isotopic ratio. Thus, the derived ratio is consistent with both standard and nonstandard evolutionary models. The lesson is clear: there is a trade-off between the need to select low-mass PNe in order to discriminate between theoretical models and the higher detection rate of molecular envelopes around more massive objects. The determination of isotopic ratios may be a tricky business, but future observations should take up such a challenge.

The method of using mm-wave transitions is not the only one adequate for measuring the isotopic abundance in PNe. Clegg (1985) first pointed out the possibility of using the CIII] multiplet near 1908 Å to obtain a direct estimate of the isotopic ratio in the *ionized* gas of PNe. Recently, Clegg et al. (1997) have successfully detected the extremely weak isotopic line ^{13}C $^3\text{P}_{1/2} - ^1\text{P}_{1/2}$ S_0 in two PNe (plus a tentative detection in a third one), using the HST Goddard High Resolution Spectrograph. The derived $^{12}\text{C}/^{13}\text{C}$ ratios are 15 ± 3 in NGC 3918 and 21 ± 11 in SMC N2. In either case, no measurement at mm-wavelengths has been made to independently check the derived values. However, as Clegg et al. point out, the two types of measurements are complementary since they cannot be performed on the same objects: the UV transitions require high excitation conditions, while the opposite is true for the mm-wave lines studied by us. Considering the negative results of the CO search, it would be extremely important to perform the HST observations towards NGC 3242.

8. Conclusions

We have observed a sample of 28 PNe in ^{12}CO and ^{13}CO . We have determined the isotopic ratio in 14 objects, 9 of which are new detections, and obtained robust upper limits in 4 other PNe. The observations reported in this paper improve the available data on the $^{12}\text{C}/^{13}\text{C}$ ratio in PNe. The results confirm and extend earlier measurements which indicate values between 5 and 30, below those predicted by current AGB models. According to these calculations, the value of $^{12}\text{C}/^{13}\text{C}$ in the ejecta of stars in the mass range between ~ 1.5 and $\sim 4 M_{\odot}$ is of the order of 100. In order to agree with the observations, we suggest that stellar nucleosynthesis models should include the effects of extra-mixing to avoid the overproduction of ^{12}C with respect to ^{13}C not only during the RGB phase, but also in the latest phases of evolution. Our estimates of the mass of the progenitor stars support this conclusion, since all PNe considered here originated from stars with mass less than $\sim 3 M_{\odot}$. The proposed extra-mixing mechanism is expected to be at work in this mass range (Hogan 1995, Charbonnel 1995) and represents at present the most likely solution to the so-called “ ^3He problem”.

Out of the six PNe with measured ^3He abundances, only for one (NGC 6720) it was possible to estimate the $^{12}\text{C}/^{13}\text{C}$ ratio. The remaining five objects show weak or no ^{12}CO emission. In the case of NGC 3242 where the ^3He measurements are the most reliable, the absence of CO emission in the envelope precludes a direct test of the predictions of stellar nucleosynthesis using millimeter line observations. We have suggested an alternative method to determine the isotopic abundance in this critical object.

We have used chemical evolution models to follow the variation with time and Galactocentric distance of the ^3He abundance and $^{12}\text{C}/^{13}\text{C}$ ratio. Whereas the model predictions for ^3He are inconsistent with the observed abundance in the Solar System and in the interstellar medium unless extra-mixing is operative in at least 90% of low-mass stars, the evolution of $^{12}\text{C}/^{13}\text{C}$ is remarkably insensitive to the effects of extra-mixing. The Galactic evolution of ^{12}C and ^{13}C is mainly governed by intermediate and massive stars, in which extra-mixing is not expected to occur.

Acknowledgements. We would like to thank M. Pérez Gutiérrez for his help with part of the observations. We acknowledge R. Rood, T. Bania and D. Balser for numerous and fruitful discussions on the ^3He measurements. We thank the referee for useful comments which improved the content of the paper. The research of F.P., M.T., and D.G has been supported by grant COFIN98-MURST at the Osservatorio di Arcetri. R.B. acknowledges partial funding from Spanish DGES grant PB96-104.

Appendix A: Notes on individual PNe

Here, we provide detailed information on the physical properties of the PNe of our sample. Unless otherwise noted, B and V magnitudes are from the Acker et al. (1992) catalogue. Fluxes, extinction constants, and diameters are from Cahn et al. (1992, hereafter CKS).

NGC 7027: The Zanstra analysis yields $\log T_{\text{eff}} = 5.28 \pm 0.02$ and $\log L/L_{\odot} = 3.66 \pm 0.03$. We have used the expansion distance from the radio image of Masson (1989). The derived mass of the central star is $M_{\text{CS}} = 0.67 M_{\odot}$.

NGC 2346: The distance, $D = 0.9$ kpc, is derived from the average extinction distance (Pottasch 1996). We obtain $\log T_{\text{eff}} = 4.76 \pm 0.01$ and $\log L/L_{\odot} = 3.80 \pm 0.04$. The mass of the central star results $M_{\text{CS}} = 0.63 M_{\odot}$.

NGC 7293: Many distance measurements are available for this nebula. Pottasch (1996) quotes a very uncertain (error up to 100%) parallax distance of $D = 0.19$ kpc. A more reliable value of $D = 0.28$ kpc comes from averaging several individual distances (Pottasch 1996). We obtain $\log T_{\text{eff}} = 5.03 \pm 0.01$ and $\log L/L_{\odot} = 1.80 \pm 0.03$ or 2.03 ± 0.03 , using the parallax and average distances, respectively. The corresponding central star masses are $M_{\text{CS}} = 0.675$ and $0.60 M_{\odot}$. The progenitor masses are 2.6 and $2.0 M_{\odot}$. Given the large error on the parallax, we prefer the latter value for the initial mass of NGC 7293.

NGC 6781: We obtain $\log T_{\text{eff}} = 4.99 \pm 0.03$. By using the statistical (CKS) and the average of individual (Acker et al. 1992) distances, we obtain respectively $\log L/L_{\odot} = 2.24 \pm 0.09$ and 2.94 ± 0.09 . In both cases, the mass of the central star coincides with the evolutionary track for $M_{\text{CS}} = 0.55 M_{\odot}$.

M 1-16: By using $D = 5.45$ kpc (CKS method with a newly measured diameter), we find $\log L/L_{\odot} = 3.36 \pm 0.14$ and $\log T_{\text{eff}} = 4.91 \pm 0.03$. The inferred mass of the central star is $M_{\text{CS}} = 0.56 M_{\odot}$.

M 1-17: With a distance of $D = 7.36$ kpc (from CKS method), we obtain $\log T_{\text{eff}} = 4.97 \pm 0.03$ and $\log L/L_{\odot} = 2.89 \pm 0.11$. The location on the HR diagram is just below the $0.55 M_{\odot}$.

M 2-9: We calculate the distance with the method of CKS, but we evaluate the effective diameter from the $H\alpha$ image ($\theta = 34.75$ arcsec). The new distance to this nebula is $D = 1.32$ kpc. No HeII flux has been detected. Thus, the Zanstra analysis gives lower limits to the temperature and luminosity. We obtain $\log T_{\text{eff}} > 4.65$ and $\log L/L_{\odot} > 2.54$ from the hydrogen recombination lines. To date, nothing has been published on this nebula to set better constraints on the mass of the central star.

M 2-51: The Zanstra analysis gives $\log T_{\text{eff}} = 5.06 \pm 0.06$ and $\log L/L_{\odot} = 2.20 \pm 0.15$. The luminosity is estimated using a distance $D = 1.92$ kpc, derived with the CKS method and a new estimate of the diameter. The resulting final mass is $M_{\text{CS}} = 0.63 M_{\odot}$.

M 4-9: The distance evaluated with the newly measured angular size based on the $H\alpha$ image by Schwarzen et al. (1992) is $D = 1.71$ kpc. For the central star, only a photographic magnitude exists. Thus, the resulting Zanstra analysis is quite uncertain. The $H\beta$ flux is from Acker et al. . The HeII flux has never been measured. We obtain $\log T_{\text{eff}} > 4.85$ and $\log L/L_{\odot} > 0.18$. A value of the mass of the central star cannot be derived.

CRL 2688: Catalogued as a “possible planetary nebula”, the famous Egg nebula is actually a proto-PN. The standard analysis via Zanstra method is not feasible, as the nebula is still very thick to optical radiation. There are two mass estimates in the literature, $M_{\text{MS}} = 1.3$ or $2.7 M_{\odot}$ respectively, which depend on the assumed mass loss rate (Sahai et al. 1998).

CRL 618: The HeII flux is not available. Therefore, we cannot derive a Zanstra temperature. Hydrogen recombination lines give $\log T_{\text{eff}} > 4.48$ and a luminosity of $\log L/L_{\odot} > 1.11$, if $D = 2.81$ kpc is used. This distance has been derived with the CKS method and diameter measured by Manchado et al. (1996). No mass determination is possible.

OH 09+1.3: Another proto-PN, with no published mass to date.

IC 5117: The distance is the average of the extinction distances quoted in Acker et al. (1992). We calculate $\log T_{\text{eff}} = 4.95 \pm 0.03$ and $\log L/L_{\odot} = 3.31 \pm 0.12$. The derived mass of the central star is $M_{\text{CS}} = 0.56 M_{\odot}$.

M 1-59: Since no stellar magnitudes are available for this object, we calculate the effective temperature with the “crossover” method (Kaler 1983). We use the statistical distance $D = 2.50$ kpc from CKS, based on a new diameter measured by Manchado et al. (1996) and obtain $\log T_{\text{eff}} = 5.07 \pm 0.01$ and $\log L/L_{\odot} = 1.37 \pm 0.02$. The mass of the central star mass is $M_{\text{CS}} = 0.85 M_{\odot}$.

NGC 6853: The parallax distance quoted in Pottasch (1996) is of the best quality, so we can confidently use this value to evaluate the luminosity. From the Zanstra analysis we derive $\log T_{\text{eff}} = 5.14 \pm 0.03$ and $\log L/L_{\odot} = 2.52 \pm 0.07$, and a central mass $M_{\text{CS}} = 0.67 M_{\odot}$.

BD+30°3639: The HeII flux is not detected. Thus, we obtain lower limits to the luminosity and temperature: $\log T_{\text{eff}} > 4.68$ and $\log L/L_{\odot} > 2.70$, using the hydrogen recombination lines and the average of extinction distances from Acker et al. (1992). No mass determination is possible.

NGC 7008: We calculate $\log T_{\text{eff}} = 4.98 \pm 0.01$ and $\log L/L_{\odot} = 3.76 \pm 0.13$. The distance used is the average of the extinction distances quoted in Acker et al. (1992). The derived central mass is $M_{\text{CS}} = 0.63 M_{\odot}$.

M 1-7: The Zanstra analysis gives $\log T_{\text{eff}} = 5.05 \pm 0.04$ and $\log L/L_{\odot} = 2.43 \pm 0.15$ when using $D = 3.47$ kpc, as derived from the diameter of Manchado et al. (1996) and the method of CKS. The mass of the central star is $M_{\text{CS}} = 0.56 M_{\odot}$.

M 1-13: Since no stellar magnitudes are available for this object, we calculate the effective temperature with the “crossover” method (Kaler 1983). We use the statistical distance $D = 5.32$ kpc from CKS to obtain $\log T_{\text{eff}} = 5.35 \pm 0.03$ and $\log L/L_{\odot} = 3.70 \pm 0.26$. The central star mass is $M_{\text{CS}} = 0.71 M_{\odot}$.

References

Acker A., Ochsenbein F., Stenholm B., et al. 1992, Strasbourg–ESO Catalogue of Galactic planetary nebulae (Garching: ESO)

Anders E., Grevesse N. 1989, Geochim. Cosmochim. Acta 53, 197

Bachiller R., Bujarrabal V., Martín-Pintado J., Gómez-González J. 1989, A&A 218, 252

Bachiller R., Huggins P.J., Martín-Pintado J., Cox P. 1992, A&A 256, 231

Bachiller R., Huggins P.J., Cox P., Forveille T. 1993, A&A 267, 177

Bachiller R., Forveille T., Huggins P.J., Cox P. 1997, A&A 324, 1123

Balser D.S., Bania T.M., Brockway C.J., Rood R.T., Wilson T.L. 1994, ApJ 430, 667

Balser D.S., Bania T.M., Rood R.T., Wilson T.L. 1997, ApJ 483, 320

Balser D.S., Bania T.M., Rood R.T., Wilson T.L. 1998, ApJ 510, 759

Boothroyd A.I., Sackmann I.-J. 1999, ApJ 510, 232 (BS)

Cahn J.H., Kaler J.B., Stanghellini L. 1992, A&AS 94, 399 (CKS)

Charbonnel C. 1994, A&A 282, 811

Charbonnel C. 1995, ApJ 453, L41

Charbonnel R., do Nascimento J.D.Jr, 1998, A&A 336, 915

Clegg R.E.S. 1985, in Production and Distribution of C, N, O Elements, eds. J. Danziger, Matteucci, F., Kjar, K. (Munich: ESO), p.261

Clegg R.E.S., Storey P.J., Walsh J.R., Neale L. 1997, MNRAS 284, 348

Cox P., Omont A., Huggins P.J., Bachiller R., Forveille T. 1992, A&A 266, 420

Dearborn D.S.P., Steigman G., Tosi M. 1996, ApJ 465, 887

Denissenkov P.A., Weiss A. 1996, A&A 308, 773

Forestini M., Charbonnel C. 1997, A&AS 123, 241 (FC)

Galli D., Palla F., Ferrini F., Penco U. 1995, ApJ 443, 536

Galli D., Stanghellini L., Tosi M., Palla F. 1997, ApJ 477, 218 (GSTP)

Gardner F.F., Whiteoak J.B., 1981, MNRAS 37, 1981

Geiss J. 1993, in Origin and evolution of the elements, eds. N. Prantzos, E. Vangioni-Flam, M. Cassé (Cambridge: CUP), p.89

Gilroy K.K., Brown J.A. 1991, ApJ 371, 578

Gloeckler G., Geiss J. 1996, Nat 381, 210

Greaves J.S., Holland W.S. 1997, A&A 327, 342

Henkel C., Walmsley C.M., Wilson T.L. 1980, A&A 82, 41

Henkel C., Wilson T.L., Bieging L. 1982, A&A 109, 344

Henkel C., Gusten R., Gardner F.F. 1985, MNRAS 143, 148

Hervig G. 1996, in Stellar Evolution: what should be done, 32nd Liège Int. Astroph. Coll., eds. A. Noels, N. Grevesse (Univ. of Liège), p.441

Hogan C.J. 1995, ApJ 441, L17

Huggins P.J., Bachiller R., Cox P., Forveille T. 1996, A&A 315, 284

Kaler J. B. 1983, ApJ 271, 188

Kastner J.H., Weintraub D.A., Gatley I., Merrill K.M., Probst R.G. 1996, ApJ 462, 777

Lambert D.L., Gustafsson B., Eriksson K., Hinkle K.H. 1986, ApJS 62, 373

Langer W.D., Penzias A.A. 1993, ApJ 408, 539

de Laverny, P. & Gustafsson, B. 1998, A&A 332, 661

Likkel L., Forveille T., Omont A., Morris M. 1988, A&A 198, L1

Manchado A., Guerrero M., Stanghellini L., Serra-Ricart M. 1996, The IAC Morphological Catalog of Northern Galactic Planetary Nebulae (Tenerife: IAC)

Marigo P. 1998, PhD Thesis, University of Padua

Masson C. R. 1989, ApJ 336, 294

Mullan D. J., Linsky J. L. 1999, ApJ 511, 502

Ohnaka K., Tsuji T. 1996, A&A 310, 933

Ohnaka K., Tsuji T. 1998, A&A 335, 1018

Pilachowski C.A., Sneden C., Hinkle K., Joyce R. 1997, AJ 114, 819

Pottasch S. R. 1996, A&A 307, 561

Rood R.T., Bania T.M., Wilson T.L. 1992, Nat 355, 618

Rood R.T., Bania T.M., Wilson T.L., Balser D.S. 1995, in ESO-EIPC Workshop on the light elements, ed. P. Crane (Heidelberg: Springer), p.201

Rood R.T., Bania T.M., Balser D.S., Wilson T.L. 1998, SSRv 84, 185

Sahai R., Trauger J.T., Watson A.M., et al. 1998, ApJ 493, 301

Sandrelli S., Visco A., Tosi M. 1998, in Nuclear Astrophysics, eds. M. Arnould et al. (New York: AIP Conf. Proceedings), 425, p.581

Schwarz H. E., Corradi R.L.M., Melnik J. 1992, A&AS 96, 23

Sneden C., Pilachowski C.A., Vandenberg D.A. 1986, ApJ 311, 826

Stanghellini L., Renzini A. 1993, in IAU Symp. 155, Planetary Nebulae, eds. R. Weinberger, A. Acker (Dordrecht: Kluwer), p.473

Straniero O., Gallino R., Busso M., et al. 1995, ApJ 440, L85

Tosi M. 1996, in From Stars to Galaxies, eds. C. Leitherer, U. Fritze-von Alvensleben, J. Huchra (ASP Conf. Ser.), 98, p.299

van den Hoek L.B., Groenewegen M.A.T. 1997, A&AS 123, 305 (HG)

Wannier P.G., Sahai R. 1987 ApJ 319, 367

Wasserburg G.J., Boothroyd A.I., Sackmann I.-J. 1995, ApJ 447, L37

Weidemann V. 1987, A&A 188, 74

Weiss A., Wagenhuber J., Denissenkov P.A. 1996, A&A 313, 581

Woosley S.E., Weaver T.A. 1995, ApJS 101, 181

Wouterloot J.G.A., Brand J. 1996, A&AS 119, 439

Zweigle J., Neri R., Bachiller R., Bujarrabal V., Grewing M. 1997, A&A 324, 624